Published in final edited form as:
Neurosci Lett. 2009 November 6; 465(1): 79–84. doi:10.1016/j.neulet.2009.08.062.

Regional expression of the anesthetic-activated potassium channel TRESK in the rat nervous system

SieHyeon Yoo[#], **Jia Liu**, **Marta Sabbadini**, **Paul Au**, **Guo-xi Xie**, and **C. Spencer Yost**[*]
Department of Anesthesia and Perioperative Care, University of California, San Francisco, 513 Parnassus Avenue, Room S-261, San Francisco, CA 94143, USA

Abstract

The two-pore-domain potassium (K_{2P}) channels contribute to background (leak) potassium currents maintaining the resting membrane potential to play an important role in regulating neuronal excitability. As such they may contribute to nociception and the mechanism of action of volatile anesthetics. In the present study, we examined the protein expression pattern of the K_{2P} channel TRESK in the rat central nervous system (CNS) and peripheral nervous system (PNS) by immunohistochemistry. The regional distribution expression pattern of TRESK has both similarities and significant differences from that of other K_{2P} channels expressed in the CNS. TRESK expression is broadly found in the brain, spinal cord and dorsal root ganglia (DRG). TRESK expression is highest in important CNS structures, such as specific cortical layers, periaqueductal gray (PAG), granule cell layer of the cerebellum, and dorsal horn of the spinal cord. TRESK expression is also high in small and medium sized DRG neurons. These results provide an anatomic basis for identifying functional roles of TRESK in the rat nervous system.

Keywords

background potassium current; K_{2P} channel; tissue distribution; CNS; dorsal root ganglia; nociception; general anesthesia; immunolocalization

Introduction

Two-pore-domain potassium (K^+) ion channels (K_{2P}, also named KCNK) form a family of potassium-selective channel subunits that share the unique structural feature of four transmembrane domains and two pore-forming domains [6]. The fifteen mammalian members have been grouped into six subfamilies based on function and structural similarity [23]. The activity of K_{2P} channels significantly contribute to the background leak K^+ currents to help maintain the resting membrane potential of a living cell [6]. K_{2P} channels also play important roles in regulating the action potential in excitable cells such as neurons and cardiovascular cells, as well as in the development and survival of cells [12,16]. Some K_{2P} channels are regulated by neurotransmitters and G protein-coupled receptors [14], and are targets of a variety

*Corresponding author: Telephone: 415-476-5200, Fax: 1-415-476-8841, yosts@anesthesia.ucsf.edu (C.S. Yost).
[#]Current address: Department of Anesthesiology and Pain Medicine, Soonchunhyang University, College of Medicine, Cheonan, Korea

of medicinal agents including volatile and local anesthetics and respiratory stimulants [18,7, 11,3].

TRESK (TWIK RElated Spinally-expressed K channel) was the last identified member of the K_{2P} channel family. Its primary sequence consists of 384 amino acids residues in the human, 394 in the mouse and 405 in the rat [22,9,10]. TRESK passes outwardly rectifying K^+ currents and functions as a background K^+ channel. The functional properties of TRESK show that it is sensitive to changes in the extra- and intra-cellular pH [22]. It has also been demonstrated that TRESK is one of the major background K^+ channels in the spinal cord and the dorsal root ganglia (DRG) [5], and is activated by intracellular calcium [4] and volatile anesthetics in the clinical concentration range [13,10].

To further explore and understand the various functions of the K_{2P} channel family, it is essential to obtain a comprehensive knowledge of their cellular expression patterns and anatomic distributions. These data provide a spatial and temporal basis for the respective physiological functions and pharmacological actions on these potassium channels. Earlier studies of gene expression and tissue distribution of the K_{2P} channels in different species, using various approaches, have produced some conflicting results. For example, using the polymerase chain reaction (PCR) and Northern blotting Sano et al. found that human TRESK subunit is expressed solely in the spinal cord, but not in brain or other tissues [22]. In contrast, other studies have reported TRESK expression not only in the spinal cord, but also in the brain, peripheral nervous tissue, dorsal root ganglia (DRG), and other tissues [5]. As the function of this member of the K_{2P} family is still poorly understood and largely unknown, it is important to have more thorough investigation of its anatomic gene expression. In this study, we conducted an immunohistochemical analysis of the regional expression of TRESK in tissues of the rat CNS and PNS with TRESK-specific antisera. The work identifies a specific pattern of tissue expression in the nervous system that may help disclose the functional significance behind TRESK expression.

Material and Methods

Animals

All experiments using laboratory animals were conducted under protocol approved by the Institutional Animal Care and Use Committee of the University of California, San Francisco. Male Sprague-Dawley rats (Bantin and Kingman, Fremont, CA, USA) aged 2 months (weighing 200–250 g) were used as the source of tissues. They were housed at 25°C under controlled lighting conditions (12 hour light/dark cycle) with free access to food and water before the perfusion. Every effort was made to reduce the suffering of rats during experiments.

Tissue preparation

Perfusion and fixation of rats were performed according to the standard procedures [1]. Briefly, rats were deeply anesthetized with sodium pentobarbital (50 mg/kg, intraperitoneal injection), in dorsal recumbancy position secured with tape. An incision was made under the rib cage extending through the peritoneum into the thorax to expose the heart of the rat. A dose of heparin sodium (1000 unit/kg, American Pharmacological Partners, Schaumburg, IL, USA) was injected into the left ventricle to prevent blood clotting. About 200 ml of 0.1 M phosphate-buffered saline (PBS), pre-warmed to 37°C was first perfused into the circulation system through the left ventricle and drained out of the right atrium, followed by a perfusion of approximately 250 ml of fixative containing 4% formaldehyde (v/v) in 0.2 M phosphate buffer pre-cooled to 4°C. After the perfusion, tissues of brain, spinal cord and lumbar DRG were dissected, fixed for 4 hours at 4°C in the same fixative, followed by dehydration in 30% sucrose (w/v) in PBS overnight. Fixed brains were cut in coronal sections of 40 μm thickness, fixed

spinal cord segments from cervical, thoracic, lumbar and sacral regions of 20 μm thickness, and fixed DRG of 10 μm thickness on a cryostat (Leica, CM1900, Solms, Germany). Tissue sections were stored in Tris-PBS (TPBS) at 4°C.

Immunohistochemistry

Immunostaining was performed according to the avidin-biotin peroxidase method described by Hsu et al. with minor modifications [8]. Tissue sections from the brain, spinal cord and DRG were selected, at least three consecutive sections for the same anatomic structure per rat (total number of rats analyzed n = 6). Specific polyclonal antisera against TRESK (the primary antisera) were used side-by-side, each with three controls (without the primary antisera; without the secondary antibody; with the primary antisera pre-absorbed with a blocking peptide used to raise the antisera) in pretreated 12-well tissue culture plates (Becton Dickinson, Franklin Lakes, NJ, USA). Tissue sections in each well were first washed three times for 5 minutes each with wash buffer [10 mM TPBS containing 1% normal rabbit serum (Vector Laboratories, Burlingame, CA, USA) and 0.3% Triton X-100], and then were blocked for 3 hours in wash buffer containing 3% normal rabbit serum. After the blocking, the sections were incubated with 1:100 dilution of the specific primary antisera directed against rat TRESK [goat polyclonal IgG, TRESK (V-12) (catalog number: sc-51240), Santa Cruz Biotechnology, Santa Cruz, CA, USA], respectively, for 4 hours with a gentle shaking at room temperature followed by a continuous incubation at 4 C overnight. After thorough washing three times with washing buffer, sections were incubated with a biotinylated rabbit-anti-goat antibody (the secondary antibody), which uses peroxidase as the detection enzyme (Vector Laboratories, Burlingame, CA, USA) for 2 hours with a gentle shaking at room temperature. After three thorough washes, diaminobenzidine (DAB) substrate kit for peroxidase (Vector laboratories) was used to localize the peroxidase reaction product. The immunostained sections were then washed three times in PBS and mounted on glass microscopic slides, air dried and covered with a coverslip using Permount histological mounting medium (Fisher Scientific, Fair Lawn, NJ, USA).

Qualitative and quantitative analyses of specific staining

Low magnification images of 10x, 30x and 50x magnification were captured with a Leica MZFL III microscope (Wetzlar, Germany) connected to a Nikon Dxm 1200 digital camera, while high magnification images of 200x and 400x magnification were captured with a Nikon Eclipse E400 microscope (Tokyo, Japan) connected to a Nikon D300 digital camera. All images were converted to gray scale and digitalized. The stereotaxic coordinates of the coronal sections of the rat brain were determined according to the atlas of Paxinos and Watson [20]. Levels of spinal cord sections were analyzed according to Paxinos [19].

The pattern and intensity of the specific staining in each image were first analyzed qualitatively using the graded scoring system of Meberg and Routtenberg with modifications [15]. Optical intensity of a target structure was compared to other structures in the section. Structures with the highest optical intensity were scored as “+++”, while structures with only non-specific background intensity were scored as “0”. Thus, the intensity grades were designated as follows: high, +++; medium, ++; low or faint, +; not detectable, 0. Intensity of specific staining of selected regions was then analyzed quantitatively using ImageJ program (version 1.24, NIH, Bethesda, MD, USA). The optical intensity of a fixed area in a positively stained region was measured and compared with a background region of the same area on the same section, and the intensity ratio was obtained. The positively stained regions were also compared with each other.

For the analysis of immunostaining in the DRG, the sizes of DRG neurons were measured with the ImageJ program, and the cells were classified into small-, medium- and large-sized cells based on the methods of Obata et al. with modifications (small: < 300μm^2, medium: 300–600

μm^2, large: > 600 μm^2) [17]. The intensity of immunostaining was then assessed as described above.

Results

Qualitative and quantitative analyses of the staining in tissue sections from multiple animals revealed very similar results in the pattern of nervous system staining. The specific scoring system used for evaluation is described in Methods. Control experiments revealed that there was virtually no staining in the control sections in which either primary or secondary antibody was omitted (data not shown), or when the primary antisera was pre-incubated with the immunizing peptide (shown in Figure 1 and Figure 3, preabsorb control). These results demonstrate that the polyclonal antisera raised against TRESK produced specific immunostainings.

Distribution of TRESK immunostaining in the brain

TRESK protein is broadly expressed in the rat brain, with highest density seen in the dentate gyrus, amygdala, pyramidal layer of hippocampus and medial habenular nucleus of thalamus (Figure 1). Higher magnification images shown in Figure 2 show the specific staining of individual neuronal cells. At higher magnification, strong TRESK expression can be seen in the layers II–VI of cortex and in dentate gyrus and hippocampus (Figure 2). Intense TRESK immunostaining was seen across various regions of the cortex including somatosensory, motor and cingulate cortex. TRESK expression is also moderately high in the periaqueductal gray (PAG) and granule and Purkinje layers of the cerebellum (Figure 2). TRESK staining is faintly seen in the olfactory tubercles and track, nucleus accumbens, lateral globus pallidus, caudate putamen, stria medullaris (SM) of thalamus and locus ceruleus of midbrain. Quantitative assessments of the intensity of immunostainings of TRESK in the rat brain are summarized in Table 1.

Expression of TRESK in the spinal cord

The expression pattern of TRESK was also examined in sections taken from all segmental levels of the spinal cord, i.e., cervical, thoracic, lumber and sacral levels (Figure 3). TRESK is expressed in the grey matter with a highest density in the dorsal horn region, especially the superficial lamini I and II, and with a medium density in the ventral horn region of all spinal levels (Figure 3). Specific expression is more clearly in the higher magnification images of the cervical section shown in Figure 4, upper panel. Quantitative determinations of the intensities of the immunostaining of TRESK throughout the rat spinal cord are summarized in Table 2.

Expression of TRESK in the DRG

In the DRG, TRESK expression is found in almost all neurons, with greatest abundance in small diameter neurons and slightly lower expression abundance in medium and large diameter neurons (Figure 4 lower panel, Table 2).

Discussion

The present study, using an immunohistochemical approach, examined the regional and cellular expression of TRESK in the adult rat nervous system. It has demonstrated that TRESK is broadly expressed in the brain and spinal cord with significant regional differences in the level of expression within these areas of the nervous system. These findings are generally in accord with previous expression and functional studies of TRESK, and provide additional new information about their specific protein expression pattern to help understand functional roles for TRESK in the mature nervous system. We did not study TRESK expression in neonatal or young animals to determine developmental changes in TRESK expression.

Several independent expression and functional studies have demonstrated that TRESK is highly expressed in DRG neurons and constitutes one of the major background K^+ channels in DRG [5,2]. Our study here also found strong TRESK immunostaining in DRG neurons of all size classes, in agreement with the previous studies. This finding represents the most distinct expression difference between TRESK and other members of the K_{2P} family. As such TRESK may play a unique and important role in peripheral sensory perception, including nociception [2].

The regional CNS distribution of TRESK experssion demonstrated in the present study may also imply novel functions. TRESK is found abundantly expressed in the PAG and the dorsal horn superficial layers of the spinal cord, regions known to be important parts of the endogenous nociception and pain modulation pathway. These findings along with the immunostaining result in DRG strengthen the argument for TRESK involvement in nociceptive trafficking and pain pathway regulation.

These results may help resolve previously reported conflicting findings. It was initially reported that TRESK is exclusively expressed in spinal cord, suggesting that TRESK may only be involved in the regulation of membrane potential in spinal cord-specific cells [21]. Kang et al. described the identification and characterization of TRESK in mouse tissues and cell culture, and called it TRESK-2 to distinguish it from the original human isolate - TRESK-1 [9]. Subsequent studies have detected a single TRESK transcript in the brain and DRG, as well as in many peripheral tissues, such as thymus, spleen and testis [13,9,5] and provide strong evidence that TRESK-2 is the rat homolog of TRESK-1.

Our study corroborates these findings by identifying TRESK protein expression widely distributed across the rat CNS and PNS. These results suggest that TRESK may contribute broadly to the maintenance and regulation of the neuronal membrane potential and excitability in the brain, spinal cord and nervous ganglia. In this sense, TRESK is more like other K_{2P} channels with wider tissue expression patterns and argues for a broader role in regulating excitability.

In summary, using immunocytochemistry we demonstrated that TRESK protein is widely distributed in the CNS and PNS tissues. The demonstration of their anatomic distributions could help to understand better the role of TRESK in anesthesia mechanisms.

Acknowledgments

This study is supported by U.S. National Institute of Health grant GM58149 (CSY).

References

1. Ausubel, FM.; Brent, R.; Kingston, RE.; Moore, DD.; Seidman, JG.; Smith, JA.; Struhl, K. Current Protocols in Molecular Biology. San Francisco: John Wiley & Sons, Inc.; 1998.
2. Bautista DM, Sigal YM, Milstein AD, Garrison JL, Zorn JA, Tsuruda PR, Nicoll RA, Julius D. Pungent agents from Szechuan peppers excite sensory neurons by inhibiting two-pore potassium channels. Nat Neurosci 2008;11:772–779. [PubMed: 18568022]
3. Cotten JF, Keshavaprasad B, Laster MJ, Eger EI 2nd, Yost CS. The ventilatory stimulant doxapram inhibits TASK tandem pore (K_{2P}) potassium channel function but does not affect minimum alveolar anesthetic concentration. Anesth Analg 2006;102:779–785. [PubMed: 16492828]
4. Czirjak G, Toth ZE, Enyedi P. The two-pore-domain K^+ channel, TRESK, is activated by the cytoplasmic calcium signal through calcineurin. J Biol Chem 2004;279:18550–18558. [PubMed: 14981085]

5. Dobler T, Springauf A, Tovornik S, Weber M, Schmitt A, Sedlmeier R, Wischmeyer E, Doring F. TRESK two-pore-domain K^+ channels constitute a significant component of background potassium currents in murine dorsal root ganglion neurones. J Physiol 2007;585:867–879. [PubMed: 17962323]
6. Goldstein SA, Bockenhauer D, O'Kelly I, Zilberberg N. Potassium leak channels and the KCNK family of two-P-domain subunits. Nat Rev Neurosci 2001;2:175–184. [PubMed: 11256078]
7. Gray AT, Zhao BB, Kindler CH, Winegar BD, Mazurek MJ, Xu J, Chavez RA, Forsayeth JR, Yost CS. Volatile anesthetics activate the human tandem pore domain baseline K^+ channel KCNK5. Anesthesiology 2000;92:1722–1730. [PubMed: 10839924]
8. Hsu SM, Raine L, Fanger H. Use of avidin-biotin-peroxidase complex (ABC) in immunoperoxidase techniques: a comparison between ABC and unlabeled antibody (PAP) procedures. J Histochem Cytochem 1981;29:577–580. [PubMed: 6166661]
9. Kang D, Mariash E, Kim D. Functional expression of TRESK-2, a new member of the tandem-pore K^+ channel family. J Biol Chem 2004;279:28063–28070. [PubMed: 15123670]
10. Keshavaprasad B, Liu C, Au JD, Kindler CH, Cotten JF, Yost CS. Species-specific differences in response to anesthetics and other modulators by the K_{2P} channel TRESK. Anesth Analg 2005;101:1042–1049. [PubMed: 16192517]
11. Kindler CH, Yost CS. Two-pore domain potassium channels: new sites of local anesthetic action and toxicity. Reg Anesth Pain Med 2005;30:260–274. [PubMed: 15898030]
12. Lauritzen I, Zanzouri M, Honore E, Duprat F, Ehrengruber MU, Lazdunski M, Patel AJ. K^+-dependent cerebellar granule neuron apoptosis. J Biol Chem 2003;278:32068–32076. [PubMed: 12783883]
13. Liu C, Au JD, Zou HL, Cotten JF, Yost CS. Potent activation of the human tandem pore domain K channel TRESK with clinical concentrations of volatile anesthetics. Anesth Analg 2004;99:1715–1722. [PubMed: 15562060]table of contents
14. Mathie A. Neuronal two-pore-domain potassium channels and their regulation by G protein-coupled receptors. J Physiol 2007;578:377–385. [PubMed: 17068099]
15. Meberg PJ, Routtenberg A. Selective expression of protein F1/(GAP-43) mRNA in pyramidal but not granule cells of the hippocampus. Neuroscience 1991;45:721–733. [PubMed: 1837850]
16. Meuth SG, Bittner S, Meuth P, Simon OJ, Budde T, Wiendl H. TWIK-related acid-sensitive K^+ channel 1 (TASK1) and TASK3 critically influence T lymphocyte effector functions. J Biol Chem 2008;283:14559–14570. [PubMed: 18375952]
17. Obata K, Yamanaka H, Fukuoka T, Yi D, Tokunaga A, Hashimoto N, Yoshikawa H, Noguchi K. Contribution of injured and uninjured dorsal root ganglion neurons to pain behavior and the changes in gene expression following chronic constriction injury of the sciatic nerve in rats. Pain 2003;101:65–77. [PubMed: 12507701]
18. Patel AJ, Honore E, Lesage F, Fink M, Romey G, Lazdunski M. Inhalational anesthetics activate two-pore-domain background K^+ channels. Nat Neurosci 1999;2:422–426. [PubMed: 10321245]
19. Paxinos, G. The rat nervous system. Vol. 2nd Edition. San Diego: Academic Press; 1995.
20. Paxinos, G.; Watson, C. The rat brain in stereotaxic coordinates. Vol. 4th Edition. San Diego: Academic Press; 1998.
21. Sano Y, Mochizuki S, Miyake A, Kitada C, Inamura K, Yokoi H, Nozawa K, Matsushime H, Furuichi K. Molecular cloning and characterization of $K_V6.3$, a novel modulatory subunit for voltage-gated K(+) channel Kv2.1. FEBS Lett 2002;512:230–234. [PubMed: 11852086]
22. Sano Y, Inamura K, Miyake A, Mochizuki S, Kitada C, Yokoi H, Nozawa K, Okada H, Matsushime H, Furuichi K. A novel two-pore domain K^+ channel, TRESK, is localized in the spinal cord. J Biol Chem 2003;278:27406–27412. [PubMed: 12754259]
23. Yost CS. Update on tandem pore (2P) domain K^+ channels. Curr Drug Targets 2003;4:347–351. [PubMed: 12699355]

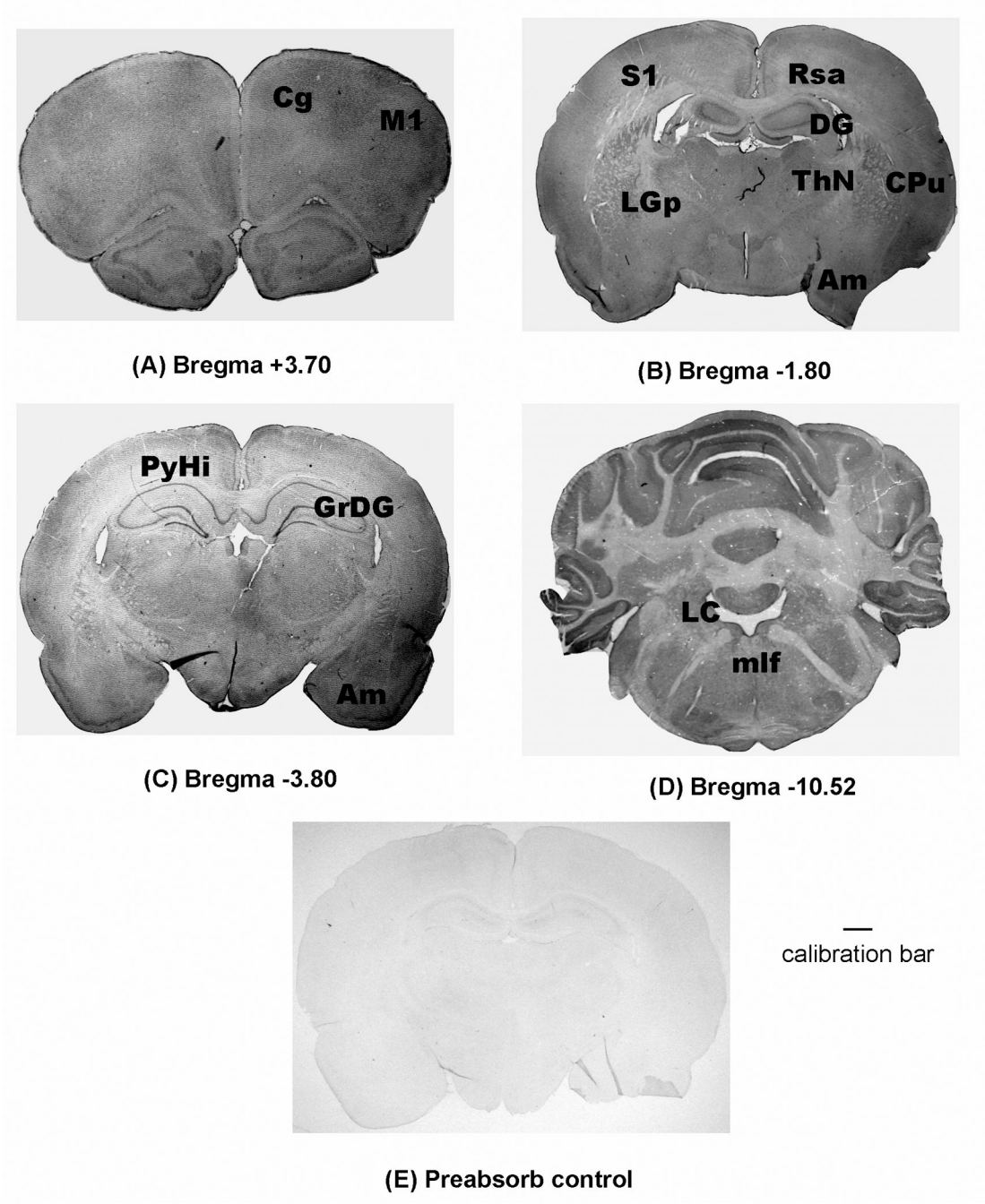

Figure 1.

Immunostaining of TRESK in the rat brain (A–C) and cerebellum (D). A control section treated with TRESK antisera that had been preabsorbed with immunizing peptide is shown in panel E. The Bregma levels of the coronal sections are determined according to the atlas of Paxinos and Watson [20]. The calibration bar represents 1 mm for all photographs. Abbreviations: Cg, cingulate cortex; M1, primary motor cortex; CPu, caudate putamen; Am, amygdala; DG, dentate gyrus; RSA, retrosplenial agranular cortex; S1, primary somatosensory cortex; ThN, thalamic nucleus; LGp, lateral globus pallidus; PyHi, pyramidal cell layer of hippocampus; GrDG, granular layer of dentate gyrus; LC, locus ceruleus; mlf, medial longitudinal fasciculus.

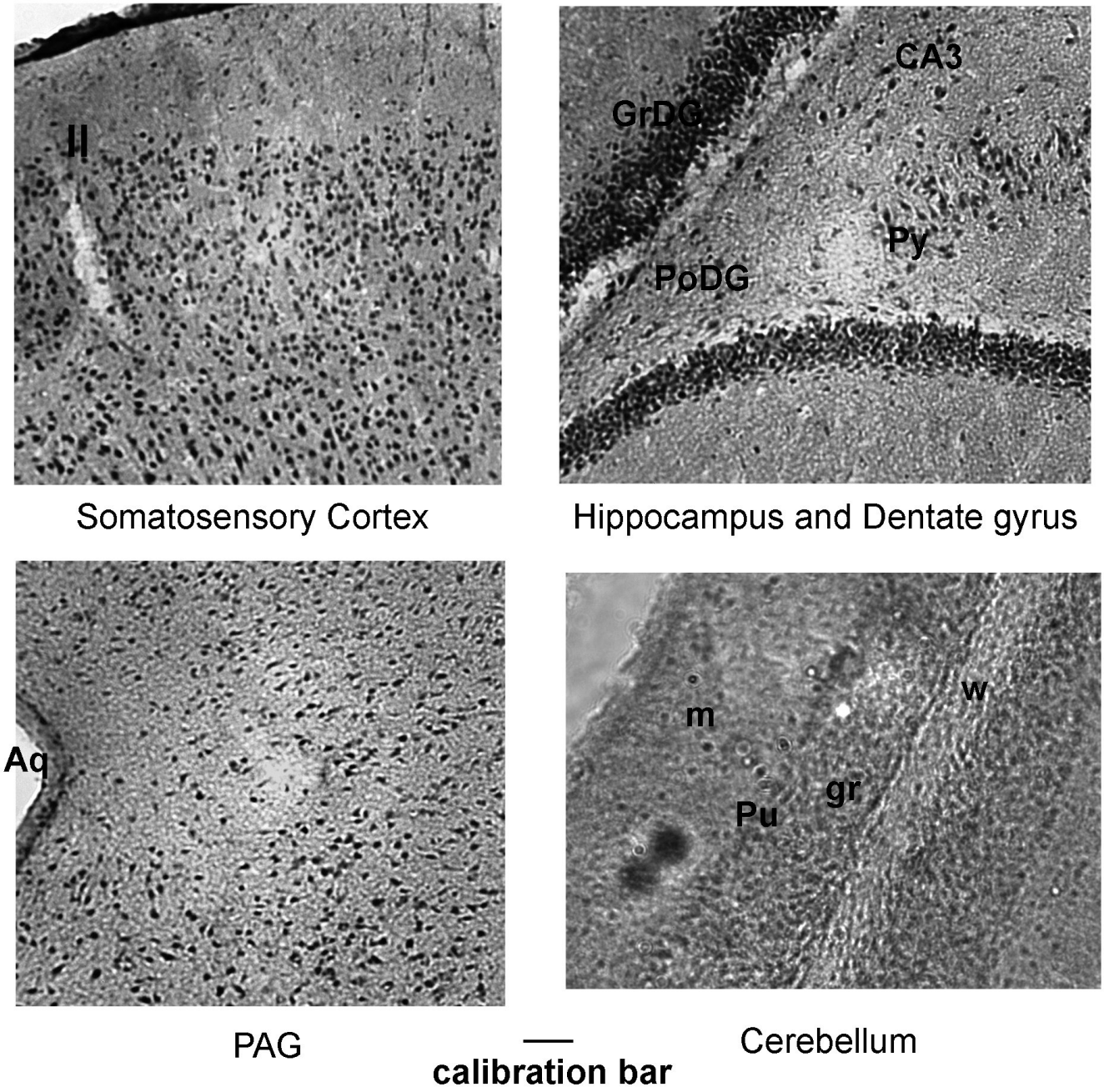

Figure 2.
TRESK expression in brain and cerebellum at higher magnification. The calibration bars represent 0.1 mm for all photographs. Abbreviations: II, layer II; PoDG, polymorph layer of dentate gyrus; Py, pyramidal cell layer of hippocampus; CA3, field CA3 of hippocampus; Aq, Sylvius aqueduct; g, granule layer; m, molecular layer; w, white matter; Pu, Purkinje layer.

Figure 3.
Immunostaining of TRESK at various levels of the rat spinal cord (low magnifications). The spinal levels are determined according to Paxinos [19]. The calibration bars represent 1 mm for all photographs. Abbreviations: C, cervical spinal cord; T, thoracic spinal cord; L, lumbar spinal cord; S, sacral spinal cord.

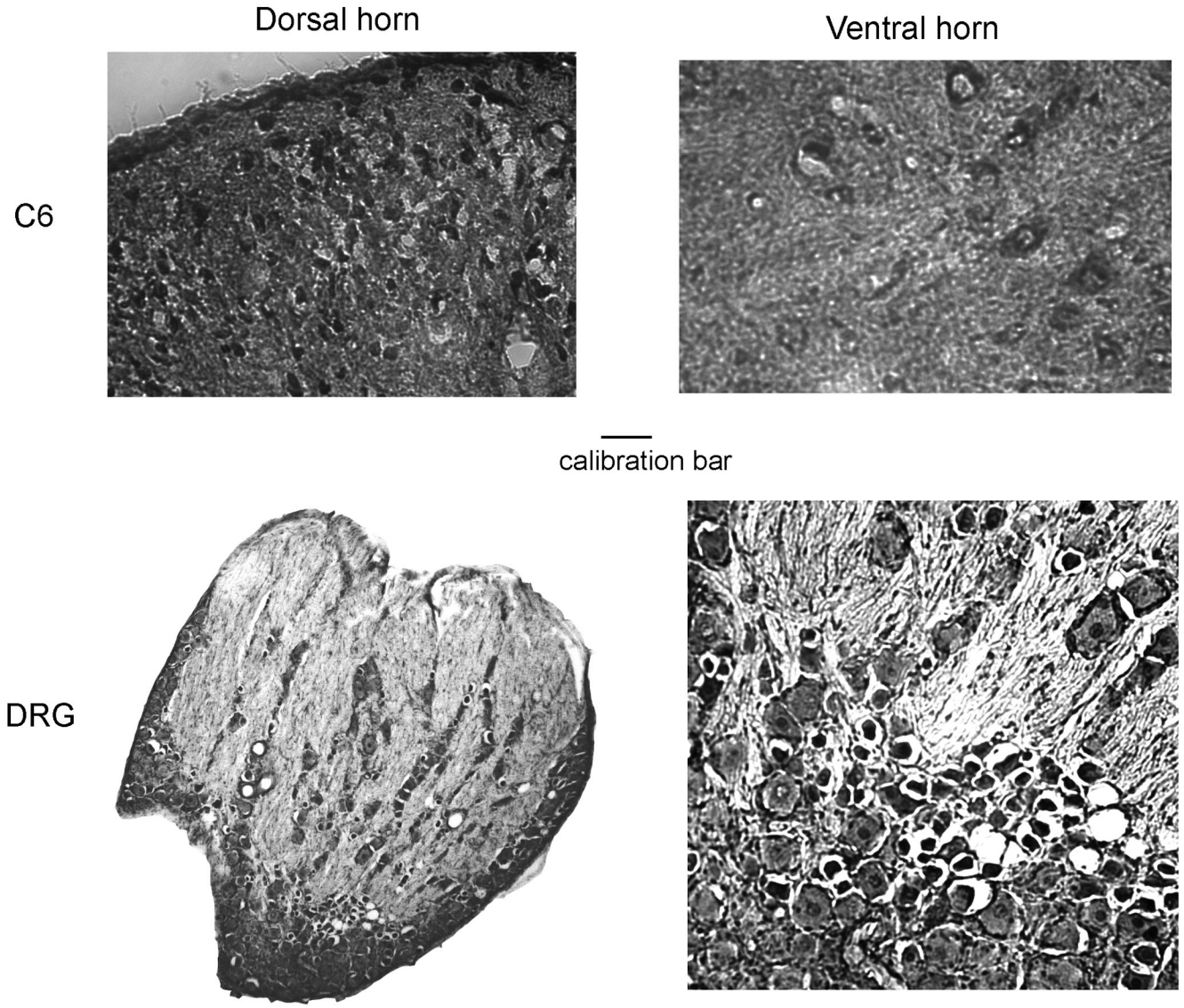

Figure 4.
Immunostaining of TRESK in rat cervical cord (high magnification) and dorsal root ganglion (low and high magnification). The calibration bar represents 0.05 mm for the high power images only. Abbreviations: C6, cervical spinal cord segment 6.

Table 1

Expression of TRESK in rat brain and cerebellum

Regions	Expression level
Motor Cortex	
Layer I	0/+
Layer II–VI	++
Cingulate and Sensory Cortex	
Layel I	0/+
Layer II	++/+++
Layer III–VI	++
Piriform Cortex	+++
Olfactory tubercles and track	+
Nucleus Accumbens	+
Lateral globus pallidus	+
Caudate putamen	+
Dentate gyrus	
Granular layer	+++
Polymorph layer	+
Molecular layer	+
Retrosplenial agranular brain cortex	
Layer I	0/+
Layer II	++/+++
Layer III–VI	++
Amygdala	++
Hippocampus	
Pyramidal cell layer	+++
CA1, CA2, CA3	0/+
Thalamus	
Lateral dorsal nucleus	++
SM	+
Anterodorsal nucleus	++
Medial habenular nucleus	++/+++
Hypothalamus	
Ventromedial nuc	++
Arcuate nucleus	++/+++
Midbrain	
Periaqueductal gray	+/++
Substantia nigra	+/++
Locus ceruleus	+
Cerebellum	
Granule layer	++
Molecular layer	+
Purkinje layer	++

Intensity of staining rated as follows: +++ highest density; ++ dense; + faint; 0 not detectable.

Table 2

Expression of TRESK in rat spinal cord and DRG

Region	TRESK
Dorsal horn	
Lamina I – III	+++
Lamina IV–VII	++
Ventral horn	
Lamina VII–IX	++
Pyramidal tract	+
IMM	++
DRG neuron size	
small	+++
medium	++
large	+/++

The table represents the common features of the regional intensity at the cervical, thoracic, lumbar and sacral spinal cord levels. Regional intensities are determined by visual inspection of black and white pictures. Intensities (visual scores) are designated as follows: the highest density, +++; dense, ++; faint, +; and not detectable, 0.

Abbreviations: LSp, lateral spinal nucleus; LatC, lateral cervical nucleus; IMM, intermediomedial cell column.